Journal of Nuclear Materials 390–391 (2009) 1035–1038

Contents lists available at ScienceDirect

Journal of Nuclear Materials

journal homepage: www.elsevier.com/locate/jnucmat

Low-energy particle interaction at carbon nanowalls on W surface

N. Tanaka [a,*], H. Yamaoka [b], M. Nishiura [c], K. Tsumori [c], T. Nagamura [a], M. Sasao [a], T. Kenmotsu [d], Y. Matsumoto [e], M. Wada [d]

[a] Tohoku University, Aramaki 6-01-2, Aoba, Sendai 980-8579, Japan
[b] Harima Institute, RIKEN (The Institute of Physical and Chemical Research), Hyogo 679-5148, Japan
[c] National Institute for Fusion Science, Toki, Gifu 509-5292, Japan
[d] Doshisha University, Kyotanabe, Kyoto 610-0321, Japan
[e] Tokushima Bunri University, Yamashiro, Tokushima 770-8514, Japan

ARTICLE INFO

PACS:
68.49.Sf
52.40.Hf
52.40.Mj

ABSTRACT

We measured the characteristics of the reflected particles from a carbon nanowall (CNW) deposited on a W surface following the injection of 1–2 keV H^+ and O^+ ions. The reflected ion energies and intensities indicated a contribution from multiple scattering in the target. The reflection angular dependence of the reflected ion intensities reached the maximum around the mirror angle and showed a sharp distribution, which may be attributable to the effect due to the aligned structure of the CNW. The energies and intensities of the reflected ions decreased with the time of ion bombardment. The intensities and energies of the reflected ions were, however, recovered to some degree by baking the sample, indicating the surface modification due to retention of the injected particles during the injection. We used the Monte Carlo simulation code ACAT (Atomic Collision in Amorphous Target) to study these processes theoretically and the calculated results supported the experimental results.

1. Introduction

In magnetically confined high-temperature plasma experiment devices Mo, W, and C are used as first wall materials, diverters and limiters. The plasma facing components are key issues from viewpoints of the components' lifetime against the enormous particle loads in a burning plasma and in the control of hydrogen recycling in edge plasma cooling processes [1,2]. Study on the particle reflections at the surfaces facing the plasma is important for understanding the heat deposition and particle recycling mechanisms. Systematic study of the particle reflections from polycrystalline samples has been performed [3–8]. The precise data set and studies of the fundamental processes for particle reflections, however, still seems to be inadequate for understanding the plasma interaction with materials in reactors, especially for carbon materials.

We have been developing an experimental system for studying fundamental processes of the particle interactions with solid surfaces [9–14]. This system successfully yielded data on reflected ions and neutrals from polycrystalline metal surfaces (Mo, C, W, V-alloy) following low-energy (1–3 keV) beam injections. The angular distributions and energy spectra of positive and negative ions reflected from the materials were measured by a magnetic momentum analyzer (MMA) [11–13]. Recently, we added a time-of-flight analyzer (TOFA) to the existing MMA so we could make complementary measurements of neutral particles during ion bombardment [14]. In this paper we report the experimental results of using the MMA-TOFA system to measure low-energy particle injection onto a carbon nanowall (CNW) coated W surface. The interactions between low-energy particles and the CNW were physically interesting because the CNW was vertically oriented to the W surface and had large porosity. Such surfaces could be present in the plasma vacuum chamber [15], and thus the study of highly oriented carbon materials is important.

2. Sample preparation and experimental setup

We prepared a CNW sample by the plasma-enhanced chemical vapor deposition on a W surface by running a 200 W RF discharge for 30 min with a H_2 and CH_4 gas mixture in a separate plasma chamber. The target W temperature was 600 °C and the substrate bias voltage was 10 V. The sample could contain hydrogen, but emits the absorbed atoms due to the high target temperature. The sample was exposed in air before being moved to the analyzer chamber of the measurement system. Example images of the CNW recorded with field-emission type secondary electron microscope (FE-SEM) are shown in Fig. 1. Vertically aligned CNW growth of a ~1 μm in thickness was observed on the W target. We could also see large empty spaces between the walls in the top view of the FE-SEM image of Fig. 1(a), and thus retention effects of the injected

* Corresponding author.
E-mail address: nozomi.tanaka@ppl2.qse.tohoku.ac.jp (N. Tanaka).

0022-3115/$ - see front matter © 2009 Elsevier B.V. All rights reserved.
doi:10.1016/j.jnucmat.2009.01.281

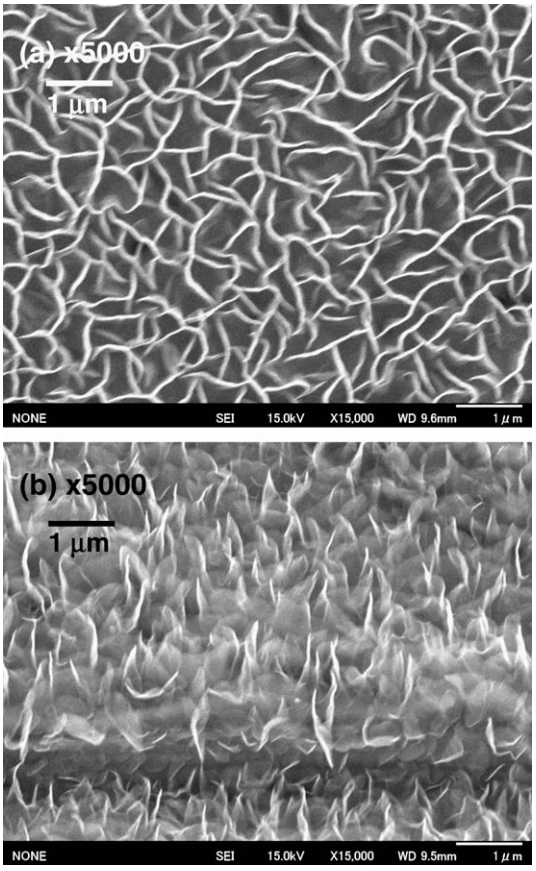

Fig. 1. Sample images of a carbon nanowall (CNW) observed by FE-SEM. A carbon nanowall (CNW) was deposited on a polished W surface. (a) Top view of the CNW. (b) Substrate tilted by 45°.

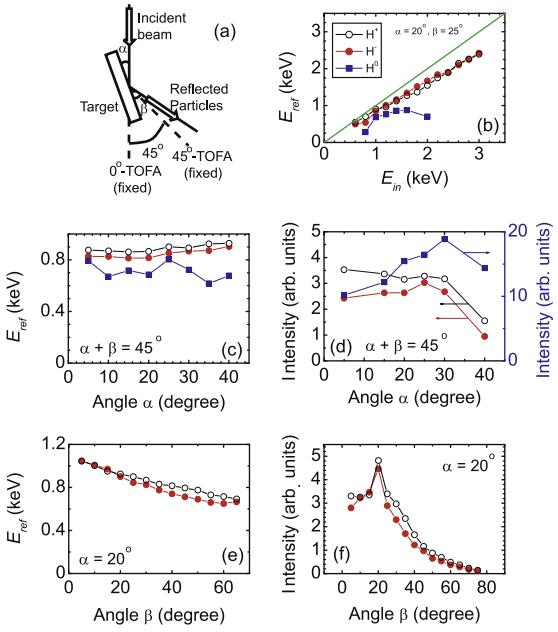

Fig. 2. Characteristics of the reflected particles for 1 keV H^+ beam injection (~50 nA for (b), ~20 nA for (c) to (f)) on the CNW target. (a) Definition of the incident angle (α) and reflected particle angle (β). (b) Incident energy dependence of the reflected particle energy at $\alpha = 20°$ and $\beta = 25°$. The solid line is a curve of $E_{in} = E_{out}$. (c) Incident angle dependence of the reflected particle energies (E_{ref}) and (d) that of the intensities under $\alpha + \beta = 45°$. (e) Reflected angle dependence of the reflected ion energies and (f) that of the ion intensities at $\alpha = 20°$. The open and closed circles correspond to the reflected H^+ and H^- ions measured by the MMA, respectively. The closed squares correspond to reflected neutral H^0 particles measured by the TOFA.

particles due to the large surface area were expected. Fig. 1(b) shows the image with the substrate tilted by 45°. The prepared CNW layer remained on the W surface after keV-beam injection with the intensity of the order of 0.5–5 mA/cm^2 for a few tens of hours. No considerable erosion of the sample was observed in the FE-SEM image after the ion bombardment.

The details of the experimental system were reported elsewhere [13,14]. The analyzer angle against the incident beam was calibrated by directly injecting the weak primary beam from the ion source to the analyzer. The correlation between the beam energy and the induction current of the magnetic momentum analyzer was carefully calibrated by directly injecting low intensity positive and negative ion beams. Our MMA system has the advantage that the positive and negative ions in the reflected beam were measured by a single sweep of the analyzer magnetic field. The target was heated by an infrared target heating system from outside the vacuum chamber through a sapphire window. We employed two fixed TOFA systems as shown in Fig. 2(a): 0°-TOFA along with the axis of the incident beam for the time calibration and 45°-TOFA aligned at 45° with respect to the incident beam [14]. The TOFA may detect the neutrals of down to a few hundreds eV. The sample temperature was measured by the system's thermocouple and correlated to the heating power of the infrared target heater, which reached approximately 240–260 °C within 10–15 min after the start of heating. The surface of the sample reached the maximum temperature much faster than did the bulk of the target. The incident beam energy was 1–2 keV, and the intensity varied from a few to nearly 100 nA.

3. Results and discussion

Fig. 2 shows the characteristics of the reflected particles for H^+ beam injection (~20 nA) on the CNW target with definitions of the incident angle (α) and reflected particle angle (β) (Fig. 2(a)). We measured the energy distributions of the reflected particles. Both peaks of H^+ and H^- measured by MMA have Gaussian-like distribution, and HWHM was ~0.5 keV.

Incident energy E_{in} dependence of the peak energy of the reflected particle E_{ref} at $\alpha = 20°$ and $\beta = 25°$ is shown in Fig. 2(b). The solid line in the figure represents a curve of no energy loss by surface reflection. The energies of reflected ions increased monotonically with the incident energy. The energies of reflected particles were smaller than those of the incident particles, due to the energy losses by multiple scattering inside the target surface layer. This trend is very similar to the ones reported for polycrystalline metal samples [13,14].

The dependence of the particle energy and intensity upon the incident angle is shown in Fig. 2(c) and (d), respectively. The beam energy was 1 keV. Here we changed only the target angle and the angle; the angle to the TOFA was fixed at 45° with respect to the beam direction, and thus $\alpha + \beta$ was kept at 45°. The mean energy of the reflected ions was larger than that of the neutrals. The reflected ion energies (E_{ref}) showed almost no dependence on the incident angle (α). The intensity of reflected neutral particles reached the maximum around $\alpha = 30°$, while the H^+ ion intensity gradually decreases with increasing incident angle up to $\alpha = 30°$, after which it decreased more rapidly to $\alpha = 40°$. These angle dependences of the intensity are very different from those observed in the other metal targets [14].

Fig. 2(e) and (f) show the reflection angle dependence of the reflected ion energies and intensities at $\alpha = 20°$. The reflected ions showed strong dependence upon the reflection angle β, and the

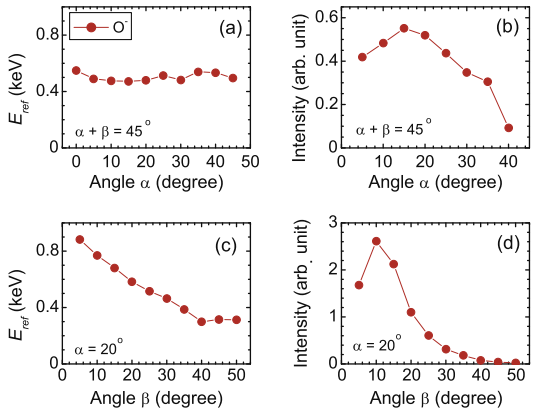

Fig. 3. Characteristics of the reflected particles for 1 keV O^+ beam injection (~6 nA) on the CNW target. (a) Incident angle dependence of the reflected O^- energy (E_{ref}) and (b) that of the intensity under $\alpha + \beta = 45°$. (c) Reflected angle dependence of the reflected O^- energy and (d) that of the intensity at $\alpha = 20°$.

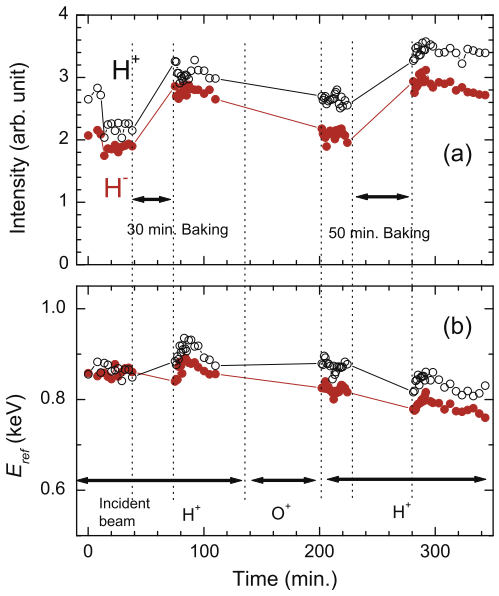

Fig. 4. Time-evolution of the reflected H^+ (opened circle) and H^- (closed circle) ions: (a) intensities and (b) energies. The incident H^+ beam energy was 1 keV. The incident and reflected angles were $\alpha = 20°$ and $\beta = 25°$, respectively. During the period of 38–75 and 225–281 min, the target was baked at about 240–260 °C.

intensity reached the maximum around the angle of mirror reflection. The reflected ions showed relatively sharp distribution for the reflection angle β compared with other metal targets [14,15], possibly due to the effect of the aligned structure of the CNW vertical to the substrate surface.

Fig. 3 shows similar measurements for a 1 keV O^+ beam injection. The energies of the reflected O^- ions showed no incident angle dependence under $\alpha + \beta = 45°$, as shown in Fig. 3(a). The energies of the reflected O^- ions were much smaller compared to the case of H^+ injection because of the similar mass of O to that of carbon. The incident angle dependence of the intensity under $\alpha + \beta = 45°$ in Fig. 3(b) shows that the angle giving the maximum intensity for the reflected O^- was around $\alpha = 15°$. Fig. 3(c) shows that the reflected angle dependence of reflected O^- ion energy was stronger than those of reflected H^+ and H^- ions. The reflected particle intensity was also strongly dependent upon the reflection angle β, taking maximum intensity around 10° as shown in Fig. 3(d).

We measured time-evolution of the reflected ions, as shown in Fig. 4. The intensities of the reflected particles drastically decreased with the time of H^+ injection in the first bombardment just after the baking. The degrees of the decrease become smaller after second bombardment. The change in the energies of reflected particles was not large, but it followed the trend of the intensity. The intensities changed most significantly just after the baking. These phenomena indicate the retention of the injected particles in the CNW. A model of one of the most possible mechanisms is described below. After the CNW retained incident beam particles, the injected beam ions collided with the absorbed particles to lose their energies efficiently by light-particle-collisions. A substantial part of the beam was not reflected, and the particle retention increased with time. The absorbed particles were reemitted from the CNW during the baking. The intensities of the reflected particles increased and the energies recovered to some degree after the beam injection was reinitiated.

To quantify the effect due to accumulation of the incident ions into the CNW, we calculated the reflection coefficients and energies from the targets by using the Monte Carlo simulation ACAT (Atomic Collision in Amorphous Target) code [16,17]. The neutral particle reflection coefficient was computed as a function of the ratio of hydrogen atoms to carbon atoms. The calculated results showed that the reflectivity and energies of the reflected particles drastically decreased as the number of absorbed hydrogen atoms in the carbon atoms increased. This may have been caused by the increase in the number of collisions with hydrogen atoms, indicating an increased elastic and inelastic energy loss in the projectiles in the materials. The calculations also show the effect of surface structure upon particles reflection coefficients and sputtering yields [18].

4. Summary

We studied low-energy beam interaction with a CNW target. The reflected H^+ and H^- intensities showed small dependence on the incident angle. This trend was different from that observed in other materials. The reflection angle dependence of the reflected ion intensities showed a sharp distribution compared to the other metal targets, indicating the effect of the aligned structure of the CNW. The reflected O^- ion energy and intensity depended strongly on the reflection angle. The time-evolution of the reflected H ions showed that the energies and intensities decreased with H^+ and O^+ beam injection time, and partly recovered as a result of baking procedures. The numerical simulation results supported these experimental results qualitatively and indicated the increased number of collisions with the hydrogen atoms absorbed in the CNW structure.

Acknowledgements

We thank Takashi Nakajima and Yohei Sakamoto for their help in the preparation of the CNW sample, and Katsuhiro Shinto of the Japan Atomic Energy Agency for his encouragement regarding performance of the experiment. This work was performed under the collaboration program of NIFS (2007 & 2008) and supported by the Iketani Science Foundation (No. 0201099-A) and a Grant in Aid for Scientific Research from Ministry of Education, Culture, Sports, Science and Technology of Japan.

References

[1] C.H. Wu, U. Mszanowski, J. Nucl. Mater. 218 (1995) 293.
[2] C.H. Wu, J. Nucl. Mater. 145–147 (1987) 448.
[3] H. Verbeek, W. Eckstein, S. Datz, J. Appl. Phys. 47 (1976) 1785.
[4] H. Verbeek, W. Eckstein, R.S. Bhattacharya, Surf. Sci. 95 (1980) 380.
[5] R. Aratari, W. Eckstein, Nucl. Instrum. and Meth. B 42 (1989) 11.

[6] M. Mayer, W. Eckstein, B.M.U. Scherzer, J. Appl. Phys. 77 (1995) 6609.
[7] S.H. Overbury, P.F. Dittner, S. Datz, R.S. Thoe, J. Nucl. Mater. 93&94 (1980) 529.
[8] K. Tsumori, W.R. Koppers, R.M.A. Heeren, M.F. Kadodwala, J.H.M. Beijersbergen, A.W. Kleyn, J. Appl. Phys. 81 (1997) 6390.
[9] M. Wada, M. Sasao, M. Nishiura, H. Yamaoka, Y. Matsumoto, Rev. Sci. Instrum. 73 (2002) 955.
[10] M. Sasao, Y. Matsumoto, A. Mendenilla, M. Nishiura, K. Shinto, M. Wada, H. Yamaoka, in: Proceedings of the Thirteenth European Physical Society International Conference on Controlled Fusion and Plasma Physics, St. Petersburg, July 2003, vol. 27A, P-2. 161.
[11] H. Yamaoka, Y. Matsumoto, M. Nishiura, K. Nishimura, M. Sasao, M. Wada, J. Nucl. Mater. 337–339 (2005) 942.
[12] H. Yamaoka, Y. Matsumoto, M. Nishiura, K. Tsumori, H. Sugawara, S. Takeuchi, K. Shinto, M. Sasao, M. Wada, Rev. Sci. Instrum. 77 (2006) 03C301.
[13] H. Yamaoka, N. Tanaka, Y. Matsumoto, M. Nishiura, K. Tsumori, H. Sugawara, S. Takeuchi, K. Shinto, A. Okamoto, M. Sasao, M. Wada, J. Nucl. Mater. 363–365 (2007) 1304.
[14] H. Yamaoka, N. Tanaka, K. Tsumori, M. Nishiura, T. Kenmotsu, M. Hirouchi, M. Kisaki, K. Shinto, M. Sasao, Y. Matsumoto, M. Wada, Rev. Sci. Instrum. 79 (2008) 02C701.
[15] S. Muto, T. Tanabe, A. Hirota, M. Rubel, V. Philipps, T. Maruyama, J. Nucl. Mater. 307–311 (2002) 1289.
[16] Y. Yamamura, Y. Mizuno, IPPJ-AM-40, Inst. Plasma Phys. Nagoya Univ., 1985.
[17] W. Takeuchi, Y. Yamamura, Radiat. Eff. Def. Solid 71 (1983) 53.
[18] T. Kenmotsu, M. Wada, H. Yamaoka, M. Nishiura, K. Tsumori, J. Plasma Fusion Res, submitted for publication.